

Langmuir–Blodgett Films of Charge-Transfer Complexes: Ethylenedithio-Substituted Amphiphilic Bis-TTF Macrocycle and F_4TCNQ or Br_2TCNQ

Toru Endo,[1] Tomoyuki Akutagawa,*[1,2] Teppei Kajiwara,[1] Keiko Kakiuchi,[1] Yoko Tatewaki,[1] Shin-ichiro Noro,[1,2] and Takayoshi Nakamura*[1,2]

[1]Graduate School of Environmental Science, Hokkaido University, Sapporo 060-0810

[2]Research Institute for Electronic Science, Hokkaido University, Sapporo 001-0020

Received March 9, 2009; E-mail: takuta@es.hokudai.ac.jp, tnaka@es.hokudai.ac.jp

Charge-transfer (CT) complexes between ethylenedithio-substituted bis-TTF macrocycle **1a**, as an amphiphilic electron donor, and 7,7,8,8-tetracyano-*p*-quinodimethane (TCNQ) derivatives, as electron acceptors, were fabricated as Langmuir–Blodgett (LB) films. For the **1a**–F_4TCNQ LB film deposited at a surface pressure of $5\,mN\,m^{-1}$ onto a substrate surface, the stoichiometry between the donor and acceptor was determined as 1:2 using XPS measurements. In contrast, a donor/acceptor ratio of 1:0.3 was observed for the **1a**–Br_2TCNQ LB film, indicating that a fraction of Br_2TCNQ was lost during the LB film formation process. Similarity of the round-shaped domains that cover the surfaces of the **1a**–Br_2TCNQ and neutral **1a** LB films indicates the presence of neutral **1a** within the **1a**–Br_2TCNQ LB film. For the $(\mathbf{1a}^{2+})(F_4TCNQ^{-})_2$ LB film, the presence of a CN-stretching frequency signifies the formation of a fully ionic electronic ground state. The LB film of **1a**–Br_2TCNQ exhibited a broad absorption at ca. $3 \times 10^3\,cm^{-1}$, which is characteristic of an intermolecular CT transition for a partial CT state. **1a**–Br_2TCNQ LB film consisted of neutral **1a** and CT complex of **1a**–Br_2TCNQ. The room temperature conductivity of the **1a**–Br_2TCNQ LB film ($1.2 \times 10^{-2}\,S\,cm^{-1}$) was two orders of magnitude higher than that of **1a**–F_4TCNQ ($3.9 \times 10^{-4}\,S\,cm^{-1}$).

Nanoscale electrically-active materials, such as dots, wires, and tubes, have been extensively investigated in the context of future nanoscale electronic devices.[1–4] Electrical properties of nanoscale dots and nanowires, along with those of carbon nanotubes have been utilized in the design of nanoscale single-electron transistors and logic gates.[4] Although nanoscale structures that are based on inorganic semiconductors have the advantage of mechanical strength, organic films of nanoscale thickness such as Langmuir–Blodgett (LB) films have attracted much attention due to their structural flexibility and ability to control their electronic structures.[5–8] Furthermore, electrically-active LB films have exhibited metallic, semiconducting, rectifying, sensing, and switching properties.[9–12] Among the several methods for introducing electrically-active units into such LB films, a relatively simple method involves the incorporation of intermolecular charge-transfer (CT) interactions between electron donor (D) and acceptor (A) molecules, which can yield the open-shell electronic structure of $(D^{\delta+})(A^{\delta-})$, where δ is the degree of CT between the D and A molecules.[13] For these $(D^{\delta+})(A^{\delta-})$-type CT assemblies, conduction carriers are generated by CT interactions, and band structures are formed through strong π–π stacking of the molecules. Because the electronic structure of the $(D^{\delta+})(A^{\delta-})$ complexes depends on the electron affinity of A and the ionization potential of D, it is possible to adjust the electronic behavior from that of partially oxidized $(D^{\delta+})(A^{\delta-})$ to fully ionic $(D^{+})(A^{-})$ states, thus directly controlling the electrical conducting properties of the CT complexes. By such precise control of the electronic structures of molecular assemblies, intermolecular CT interactions may offer novel electrically active nanoscale films.

We have recently reported the formation of molecular assembly nanowires on mica surfaces based on a methylthio-substituted amphiphilic bis(tetrathiafulvalene) [bis-TTF] macrocycle **2**, which possesses two redox-active TTF units linked via a [24]crown-8 macrocycle and two long hydrophobic decylthio-chains (Scheme 1).[14–17] The amphiphilic bis-TTF macrocycle was designed with the following considerations: i) the use of electron-donating TTF units for realizing electrically conducting π–π stacks, ii) ion-recognition at the macrocyclic moiety, and iii) incorporation of two hydrophobic alkyl chains to utilize the LB method. The fully ionic CT complex between one molecule of donor **2** and two molecules of 2,3,5,6-tetrafluoro-7,7,8,8-tetracyano-*p*-quinodimethane (F_4TCNQ) formed oriented $(\mathbf{2}^{2+})(F_4TCNQ^{-})_2$ molecular assembly nanowires, with typical dimensions of $2 \times 50 \times 1000\,nm^3$, on mica surfaces. The π-planes of the TTF system showed a tendency to form one-dimensional π–π stacking structures through CT interactions, which is typical in molecular conductors.[13] Chemical modifications of the TTF units have been shown to affect the dimensionality of intermolecular interactions, along with the molecular assembly and electronic structures of the CT complexes. Accordingly, we have recently synthesized a novel ethylenedithio-substituted amphiphilic bis-TTF macrocycle **1a**,[18] in which the methylthio substituent of the TTF unit was switched with an ethylenedithio moiety resulting in significant

Published on the web August 7, 2009; doi:10.1246/bcsj.82.968

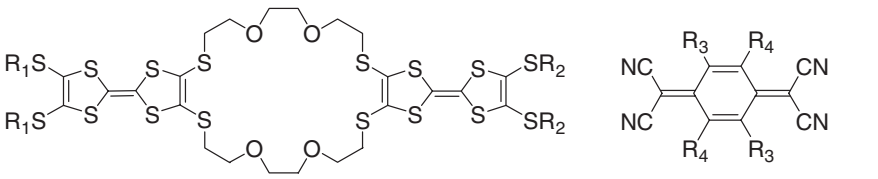

1a: R_1 - R_1 = CH_2CH_2, R_2 = $C_{10}H_{21}$
1b: R_1 - R_1 = CH_2CH_2, R_2 - R_2 = CH_2CH_2
2: R_1 = CH_3, R_2 = $C_{10}H_{21}$

F_4TCNQ: R_3 = R_4 = F
Br_2TCNQ: R_3 = Br, R_4 = H

Scheme 1. Molecular structures of bis-TTF macrocycles **1a**, **1b**, and **2** and TCNQ derivatives (F_4TCNQ and Br_2TCNQ).

changes in the molecular assembly nanostructures. Although the ethylenedithio group was expected to increase the dimensionality of the intermolecular interactions through lateral sulfur–sulfur contacts, molecular assemblies such as organogels and nanodots were formed.[18] LB films based on the CT complexes of donor **1a**, therefore, can potentially form novel electrically active nanostructures. Herein, we report the fabrication of such LB films between donor **1a** and electron acceptors F_4TCNQ and 2,5-dibromo-TCNQ (Br_2TCNQ), in which the electronic structures of the LB films were dependent on the electron affinity of the acceptor molecules. Furthermore, the results were compared to those of crystalline (**1b**)(F_4TCNQ)$_2$ and (**1b**)(Br_2TCNQ)$_2$.

Experimental

Polarized UV–vis–NIR (300–3000 nm) and IR (400–7800 cm^{-1}) spectra were measured using Perkin-Elmer Lamda-19 and Perkin-Elmer Spectrum 2000 spectrometers, respectively. Redox potentials of the samples were measured as 0.1 mM solutions in anhydrous 1,2-dichloroethane, with 0.1 M (n-Bu_4N)(BF_4) as the supporting electrolyte, using platinum (working and counter electrode) and saturated calomel electrodes (SCE) as references. The scan rate was 20 mV s^{-1}. Monolayers and LB films were formed using a conventional LB trough (NIMA 632D1D2) equipped with two symmetric moving barriers. Subphases of milli-Q (>18 MΩ) and aqueous 0.01 M KCl were employed. Hydrophobic treatments of CaF_2 and quartz substrates were carried out using a five-layer deposition of Cd^{2+}–arachidate at a constant surface pressure (30 mN m^{-1}). AFM images were obtained using a Seiko SPA 400 with an SPI 3800 probe station operating at a dynamic force mode. Commercially available Si cantilevers with a force constant of 13 mN m^{-1} were used.

Materials. Syntheses of donors **1a** and **1b** were carried out following a stepwise protection–deprotection protocol of cyanoethylene groups. Details of the synthetic procedures have been reported elesewhere.[18] The (**1b**)(F_4TCNQ)$_2$ and (**1b**)(Br_2TCNQ)$_2$ crystals were prepared using donor **1b** in 1,2-dichloroethane and three equivalents of TCNQs in CH_3CN (or benzene) following a standard mixing method. 1,2-Dichloroethane and CH_3CN were distilled from CaH_2. The (**1b**)(IBr_2)$_2$(CH_2Cl_2)$_4$ crystals were grown in an H-shape cell (ca. 18 mL) following the standard electrocrystallization method. The supporting electrolyte of [n-(C_4H_9)$_4$N]-(IBr_2) was purchased from Tokyo Kasei, Inc., and was used without further purifications. A constant current (1 μA) was applied to the platinum electrodes (1 mm ϕ) for three weeks at rt. Elemental analysis of (**1b**)(F_4TCNQ)$_2$: Calcd for $C_{52}H_{32}O_4N_8F_8S_{16}$: Calcd. C, 41.70; H, 2.15; N, 7.48%. Found. C, 41.34; H, 2.20; N, 7.44%. (**1b**)(Br_2TCNQ)$_2$(CH_3CN): Calcd for $C_{54}H_{39}O_4N_9Br_4S_{16}$: C, 37.92; H, 2.30; N, 7.37%. Found. C, 37.76; H, 2.38; N, 7.46%.

Preparation of LB Films. CT complexes **1a**–F_4TCNQ and **1a**–Br_2TCNQ were prepared in situ by mixing donor **1a** and two equivalents of F_4TCNQ or Br_2TCNQ, respectively, in $CHCl_3$/CH_3CN (8:2, v/v). Concentration of the spreading solution was fixed at 1 mM with respect to **1a**. Isotherms of surface pressure (π)–area per molecule (A) were recorded at 291.5 K with a barrier speed of 100 cm^2 min^{-1} After spreading of the CT complexes, the floating monolayers were allowed to stand for 30 min. The LB monolayers were transferred onto freshly cleaved mica surfaces at a fixed surface pressure of 5 mN m^{-1} by a single up-stroke drawing. For spectroscopic measurements, the horizontal lifting method was employed for deposition of the samples on hydrophobic substrates. The 40-layer LB films were transferred onto a quartz surface for UV–vis–NIR spectroscopy, and onto CaF_2 and evaporated gold substrates (20 × 13 mm^2) for IR transmittance spectral measurements.

Electrical Conductivity Measurements. Temperature-dependent electrical conductivity of 40-layer LB film on poly(ethylene telephthalate) (PET) film was determined using the dc two-probe method. Gold electrodes with an electrode gap of 500 μm were formed by vacuum evaporation. Electrical contacts were prepared using silver paste to attach the 25-μmϕ gold wires. Electrical conductivities were calculated assuming a single LB layer height of 2.5 nm.

X-ray Photoelectron Spectra. XPS measurements were carried out on a JEOL JPS-9200 spectrometer, with Al Kα (1486.6 eV) radiation at 293 K, using 20- or 40-layer LB films on Au substrates. Stoichiometry between the donors and acceptors on the films was estimated from the ratio of the signal intensities of S (S2p, ca. 163 eV) for donor **1a** and N (N1s, ca. 398 eV) for acceptors (F_4TCNQ and Br_2TCNQ).

Results and Discussion

Floating Monolayers at the Air–Water Interface. The π–A isotherms of a floating monolayer of neutral **1a** and CT complexes on an aqueous 0.01 M KCl subphase (T = 291.5 K) are shown in Figure 1. Formation of stable floating monolayers was confirmed by the sharp increases in the surface pressure during compression. As shown in Figure 1, the surface areas of neutral **1a**, **1a**–F_4TCNQ, and **1a**–Br_2TCNQ extrapolated at 0 mN m^{-1} were A_0 = 0.65, 1.38, and 1.12 nm^2, respectively, while those at 5 mN m^{-1} (A_5) were 0.62, 1.25, and 1.04 nm^2, respectively. The cross-sectional area of neutral **1a** at 5 mN m^{-1} (A_5 = 0.62 nm^2) was slightly larger than the sum of two alkyl chains (0.25 × 2 = 0.5 nm^2),[5] suggesting that the area of the floating monolayer was fundamentally dominated by the two decylthio chains of **1a**.

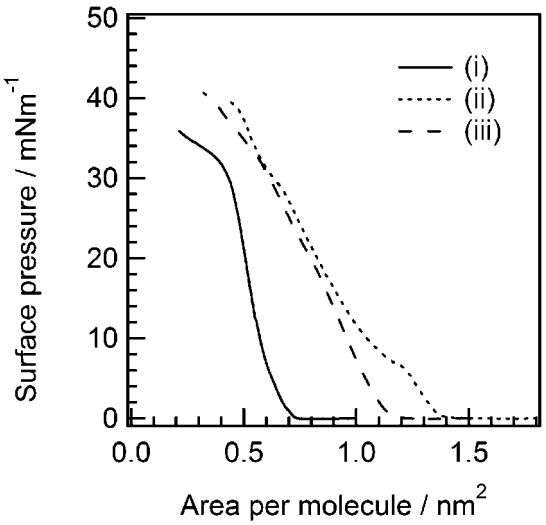

Figure 1. π–A isotherms of (i) **1a** (solid line), (ii) **1a**–F_4TCNQ (dot line), and (iii) **1a**–Br_2TCNQ (dash line) on aqueous 0.01 M KCl subphase.

The A_0 value of **1a**–F_4TCNQ was about 0.75 nm^2 greater than that of neutral donor **1a**, and about 0.25 nm^2 greater than that of **1a**–Br_2TCNQ. Because the Connolly surface areas (van der Waals area on the π-plane) of the F_4TCNQ (0.20 nm^2) and Br_2TCNQ (0.23 nm^2) molecules are comparable, the molecular assembly structures of **1a**–Br_2TCNQ and **1a**–F_4TCNQ should significantly differ at the air–water interface ($\pi < 8$ mN m^{-1}). Alternatively, it is possible that some Br_2TCNQ was dissolved into the subphase during the formation of the monolayers. Although an inflection point of the π–A isotherms for **1a**–F_4TCNQ was observed at around 8 mN m^{-1}, comparable surface areas were observed for the floating monolayers of **1a**–Br_2TCNQ and **1a**–F_4TCNQ above the surface pressure of 15 mN m^{-1}. The structure and properties of LB films deposited at 5 mN m^{-1} were characterized.

Structure of LB films. Stoichiometries of the LB films were determined based on the relative signal intensities of the S atoms of **1a** and N atoms of F_4TCNQ or Br_2TCNQ. If the ratio between the donor and acceptor in the original mixture was similarly maintained in the LB films, the signal intensities of the S and N atoms should reflect the ratio between sixteen S and eight N atoms. In the case of the **1a**–F_4TCNQ LB film, the intensities of the sulfur (S2p) and nitrogen (N1s) peaks indicated that the **1a**:F_4TCNQ ratio of 1:2 was maintained. In contrast, the **1a**–Br_2TCNQ LB film exhibited a **1a**:Br_2TCNQ ratio of 1:0.3, indicating that a fraction of Br_2TCNQ was lost during the film formation (Figure S1 in Supporting Information).

AFM images of the LB films of **1a**–F_4TCNQ and **1a**–Br_2TCNQ transferred onto freshly cleaved mica by a single withdrawal are shown in Figure 2. The monolayers were transferred at a surface pressure of 5 mN m^{-1} from the 0.01 M KCl subphase. Although the transferred films of $(\mathbf{2}^{2+})(F_4TCNQ^-)_2$ have resulted in the formation oriented molecular assembly nanowires, with typical dimensions of $2 \times 50 \times >1000$ nm^3,[17] the LB films of **1a**–F_4TCNQ and **1a**–Br_2TCNQ did not exhibit the formation of molecular nanowires on mica surfaces. As shown in Figures 2a and 2b, relatively uniform surfaces,

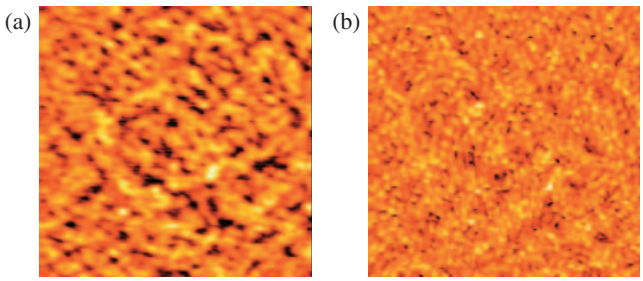

Figure 2. Surface morphology of LB films of (a) **1a**–F_4TCNQ and (b) **1a**–Br_2TCNQ, transferred onto a mica surface by a single withdrawal from an aqueous 0.01 M KCl subphase ($\pi = 5$ mN m^{-1}). The images of (a) and (b) are taken over a 2×2 μm^2 scanning area.

with average heights of ca. 1 nm, were observed for the 2×2 μm^2 LB films of **1a**–F_4TCNQ and **1a**–Br_2TCNQ. Because the surface morphologies between the **1a**–F_4TCNQ and $(\mathbf{2}^{2+})(F_4TCNQ^-)_2$ LB films were drastically dissimilar, it can be assumed that the ethylenedithio substituent of **1a** enhances the dimensionality of the intermolecular interactions, resulting in a relatively uniform two-dimensional isotropic surface, compared to that of $(\mathbf{2}^{2+})(F_4TCNQ^-)_2$.

The AFM image (Figure 2b) of **1a**–Br_2TCNQ LB film indicates the presence of round-shaped domains, with typical dimensions of $80 \times 80 \times 1$ nm^3, over most of its surface. We have previously presented the AFM image of the neutral **1a** LB film (Figure S2 in Supporting Information), which showed an aggregation of round-shaped domains. The similarity between the AFM images strongly suggests that the presence of neutral **1a** within the **1a**–Br_2TCNQ LB film, which is consistent with the those of XPS measurements.

Electronic Structures of the LB Films. Amphiphilic bis-TTF macrocycle derivatives **1a** and **1b** possess two reversible redox processes with $E_{1/2}(1) = 0.58$, $E_{1/2}(2) = 0.93$ V and $E_{1/2}(1) = 0.59$, $E_{1/2}(2) = 0.94$ V, respectively. The resemblance of the redox processes indicates comparable electron donating abilities for donors **1a** and **1b** (Figure S3 in Supporting Information). Under similar conditions, typical electron donors such as TTF and bis(ethylenedithio)-TTF (BEDT-TTF) exhibited $E_{1/2}(1)$ values of 0.50 and 0.63 V, respectively, and therefore, the electron donating abilities of **1a** and **1b** are higher than that of BEDT-TTF while lower than that of TTF.

The UV–vis–NIR and IR electronic spectra of the **1a**–F_4TCNQ and **1a**–Br_2TCNQ LB films were measured to evaluate their electronic ground states. As shown in Figure 3a, the shape of the electronic spectra of the **1a**–F_4TCNQ and **1a**–Br_2TCNQ LB film were significantly different. To help assign each absorption band, the electronic spectra of crystalline CT complexes of **(1b)**$(F_4TCNQ)_2$, **(1b)**$(Br_2TCNQ)_2$, and $(\mathbf{1b}^{2+})(IBr_2^-)_2$ (Figure 3b, spectra i, ii, and iii, respectively) were obtained as KBr pellets. To assign the CT transition of the di-cationic radical state of $\mathbf{1b}^{2+}$, the absorption behavior of the fully ionic $\mathbf{1b}^{2+}$ was identified using the electronic spectrum of $(\mathbf{1b}^{2+})(IBr_2^-)_2$.

Because the electronic spectrum of the **1a**–F_4TCNQ LB film was essentially equivalent to that of the crystalline **(1b)**$(F_4TCNQ^-)_2$ complex, it can be suggested that these

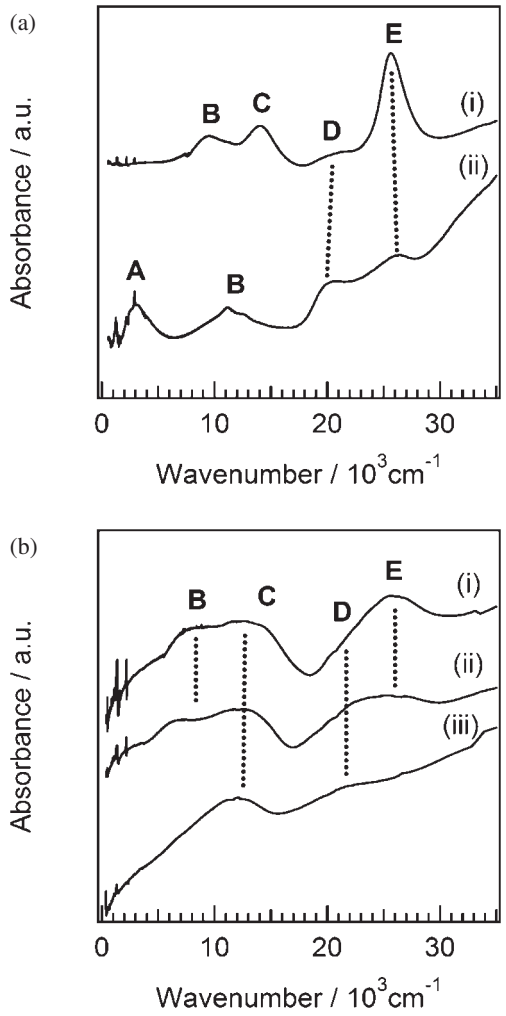

Figure 3. UV–vis–NIR–IR spectra of CT complexes. (a) 40-layer LB films of (i) **1a**–F_4TCNQ and (ii) **1a**–Br_2TCNQ transferred from an aqueous 0.01 M KCl subphase ($\pi = 5\,mN\,m^{-1}$). (b) Absorption spectra of crystalline CT complexes of (i) (**1b**)$(F_4TCNQ)_2$, (ii) (**1b**)$(Br_2TCNQ)_2$, and (iii) $(\mathbf{1b}^{2+})(IBr_2^-)_2$ as KBr pellets. Assignments of bands **A**–**E** are described in the text.

molecular assemblies are similar in electronic ground state and packing structure. Absorption maxima for the **B**- and **C**-bands of **1a**–F_4TCNQ and $(\mathbf{1b}^{2+})(F_4TCNQ)_2$ were observed at 9.6 and $14.0 \times 10^3\,cm^{-1}$, respectively. The electronic absorption spectrum of fully ionic $(Na^+)(F_4TCNQ^-)$ salt exhibited a broad CT absorption at ~$7 \times 10^3\,cm^{-1}$,[19] in which the corresponding energy was consistent with that of the **B**-bands for **1a**–F_4TCNQ LB film and (**1b**)$(F_4TCNQ)_2$. The electronic ground state of F_4TCNQ in both molecular assemblies can, therefore, be assigned to the fully ionic F_4TCNQ^-. The cation radical of $(\mathbf{1b}^{2+})(IBr_2^-)_2$ exhibited a broad **C**-band at ca. 12.8×10^3 cm^{-1}. Based on the crystal structures of the bis-TTF macrocycle derivatives,[20,21] donor $\mathbf{1b}^{2+}$ possesses a tendency to adopt the *Z*-type conformation, in which intramolecular π-dimers of two TTF^+ units were confirmed. The **C**-band absorption of $(\mathbf{1b}^{2+})(IBr^-_2)_2$ was assigned to the intramolecular CT transition between two TTF^+ units within donor $\mathbf{1b}^{2+}$. The appearances of both **B**- and **C**-bands of **1a**–F_4TCNQ in the LB film and crystalline (**1b**)$(F_4TCNQ)_2$ were consistent with the fully ionic electronic ground states of $(\mathbf{1a}^{2+})(F_4TCNQ^-)_2$ and $(\mathbf{1b}^{2+})(F_4TCNQ^-)_2$, respectively. The **D**-band ($21 \times 10^3\,cm^{-1}$) and **E**-band ($25 \times 10^3\,cm^{-1}$) were assigned to the intramolecular transitions of TTF^+ and F_4TCNQ^-, respectively.

The **1a**–Br_2TCNQ LB film exhibited a broad **A**-band at ca. $3 \times 10^3\,cm^{-1}$, which is characteristic of the intermolecular CT transition ($h\nu_{CT}$) of a partial CT state.[22] According to the electronic spectrum of $(\mathbf{1a}^{2+})(F_4TCNQ^-)_2$, the energy of the CT transition for the fully ionic electronic ground state appeared at a significantly higher energy region (ca. $10 \times 10^3\,cm^{-1}$) due to Coulomb repulsive energy. Although the electronic spectrum of crystalline (**1b**)$(Br_2TCNQ)_2$ complex was similar to that of $(\mathbf{1b}^{2+})(F_4TCNQ^-)_2$, the shape of the absorption spectrum for the **1a**–Br_2TCNQ LB film was entirely different from that of the crystalline CT complex. Because the CT transition of the fully ionic $(K^+)(Br_2TCNQ^-)$ salt was observed at $6.5 \times 10^3\,cm^{-1}$, the **B**-band of (**1b**)$(Br_2TCNQ)_2$ was assigned to the fully ionic ground state of Br_2TCNQ^-. The **C**-band at $12.3 \times 10^3\,cm^{-1}$ for (**1b**)$(Br_2TCNQ)_2$ was also consistent with the intramolecular CT transition of $\mathbf{1b}^{2+}$ with a *Z*-type molecular conformation. The electronic structure of fully ionic $(\mathbf{1b}^{2+})(Br_2TCNQ^-)_2$ was, therefore, realized in the crystalline CT complex. In contrast, it can be assumed that partial CT states between **1a** and Br_2TCNQ exist in the LB film. Moreover, the electronic spectrum of the **1a**–Br_2TCNQ LB film exhibited significantly lower intensity of the **E**-band (corresponding to the intramolecular transition of Br_2TCNQ^-) compared to crystalline (**1b**)(Br_2TCNQ), which indicates the dissolution of the Br_2TCNQ and/or Br_2TCNQ^- species during the film formation.

Next, we will discuss the electronic ground state of the LB films based on the difference in the redox potentials, $\Delta E = E_{1/2}(\mathbf{1a}) - E_{1/2}(\text{TCNQs})$, between electron donor **1a** and electron acceptors F_4TCNQ and Br_2TCNQ, and explain the origin of the **A**-bands in the electronic absorption spectra. Although the redox potentials in solution are affected by solvation energies,[23] the relative strength of the electron affinity of the TCNQ derivatives can be predicted using the first reduction potential $E_{1/2}(1)$.[24,25] Assuming similar solvation energies among all TCNQ derivatives, and based on the $E_{1/2}(1)$ values of F_4TCNQ (0.75 V) and Br_2TCNQ (0.56 V) (Figure S3 in Supporting Information), the electron affinity of F_4TCNQ should be about 0.2 eV lower than that of Br_2TCNQ. To date, two methods have been proposed for predicting the electronic ground state of CT complexes based on ΔE. Under the method of Saito et al.,[24] a partial CT state of $(D^{\delta+})(A^{\delta-})$ with $0.5 < \delta < 1$, which is necessary for metallic CT complexes with segregated-stack structures, is achieved under the condition of $-0.02 < \Delta E < 0.34$ V, in which fully ionic $(D^{1+})(A^{1-})$ or neutral $(D^0)(A^0)$ complexes are typically observed when $\Delta E < -0.02$ V and $\Delta E > 0.34$ V, respectively. In contrast, the method of Torrance et al.[25] can be applied to mixed-stack $(D^{\delta+})(A^{\delta-})$ complexes, in which a phase boundary between ionic $(D^{1+})(A^{1-})$ and neutral $(D^0)(A^0)$ complexes is observed at ca. $\Delta E = 0.17$ V, in which fully ionic $(D^{1+})(A^{1-})$ and neutral $(D^0)(A^0)$ ground states are typically observed when $\Delta E < 0.17$ V and $\Delta E > 0.17$ V, respectively. Because the ΔE

value for **1a**–F_4TCNQ (−0.17 V) was within the range of fully ionic ground state under both methods, it is reasonable to assume an electronic ground state of $(\mathbf{1a}^{2+})(F_4TCNQ^{-})_2$, whether the packing structure of **1a**–F_4TCNQ exists as a segregated- or mixed-stack structure. On the other hand, the ΔE value for **1a**–Br_2TCNQ (+0.02 V) indicates that the electronic ground state depends on the packing structure of **1a** and Br_2TCNQ. If the packing structure exists as a mixed-stacked D–A type, the electronic ground state should be that of a fully ionic $(\mathbf{1a}^{2+})(Br_2TCNQ^{-})_2$, according to the method by Torrance. If, on the other hand, the packing structure of the CT complex exists as a segregated-stack structure, the electronic ground state would be that of a partial CT state, according to the method by Saito. Because the $h\nu_{CT}$ value (ca. $3 \times 10^3\,cm^{-1}$) was significantly lower than that of the theoretical limit of minimum CT transition energy (ca. $5 \times 10^3\,cm^{-1}$, as proposed by Torrance), both segregated-stacking structure and partial CT are expected for the **1a**–Br_2TCNQ LB film.

Vibrational Spectra of LB Films. The electronic states of F_4TCNQ and Br_2TCNQ within the LB films were evaluated using the CN-stretching vibrational mode (ν_{CN}) in the IR spectra. It has been reported that the energy of the ν_{CN}-band for the TCNQ derivatives is sensitive to the charge on the TCNQ molecule. One-electron reduction of TCNQ would change the resonance structure from that of a quinonoide to an aromatic, causing a red-shift of the ν_{CN} mode through the ionization. The transmission (T) IR spectra of the **1a**–F_4TCNQ and **1a**–Br_2TCNQ LB films on CaF_2 substrate are shown in Figures 4a and 4b, respectively.

The ν_{CN}-band of **1a**–F_4TCNQ in the LB film and $(\mathbf{1b}^{2+})(F_4TCNQ^{-})_2$ in the crystalline CT complex were observed at 2195 and 2193 cm^{-1}, respectively, and can be assigned to the a_g-mode of fully ionized F_4TCNQ^{-}.[26] Although the a_g-mode is usually forbidden in the IR spectra, lattice distortions such as dimerization of F_4TCNQ can activate the a_g-mode due to the loss of symmetry within the molecular environment. Using X-ray crystallography, structural analysis of $(\mathbf{1b}^{2+})(F_4TCNQ^{-})_2$ revealed the formation of strongly interacting F_4TCNQ dimers within the crystal. In comparison, neutral F_4TCNQ^0 and ionized $Na^+(F_4TCNQ^{-})$ exhibited ν_{CN} (a_g) bands at 2227 and 2195 cm^{-1}, respectively, whereas the fully ionic (dibenzo-TTF^+)(F_4TCNQ^{-}) complex exhibited an a_g-mode at 2193 cm^{-1},[27] which is in agreement to the energy associated to **1a**–F_4TCNQ. The electronic ground state of F_4TCNQ, therefore, can be described as that of the fully ionic electronic state of F_4TCNQ^{-}.

The main ν_{CN}-bands of the **1a**–Br_2TCNQ LB film were observed at 2182 and 2162 cm^{-1} (Figure 4b, line i). Unfortunately, assignments of the three ν_{CN}-bands with symmetries of b_{1u}, a_g, and b_{2u} for Br_2TCNQ were ambiguous due to low symmetry of the molecular structure, and small amount of reference data. In the cases of TCNQ and F_4TCNQ, three types of ν_{CN}-bands, in the energy order of b_{1u}-, a_g-, and b_{2u}-bands, were observed. Although neutral Br_2TCNQ exhibited two ν_{CN}-bands (2219 and 2208 cm^{-1}), the fully ionic $K^+(Br_2TCNQ^{-})$ exhibited three ν_{CN}-bands (2193, 2180, and 2164 cm^{-1}). Because crystalline $(\mathbf{1b}^{2+})(Br_2TCNQ^{-})_2$ CT complex exhibited a ν_{CN}-band (2176 cm^{-1}) that was comparable to the second

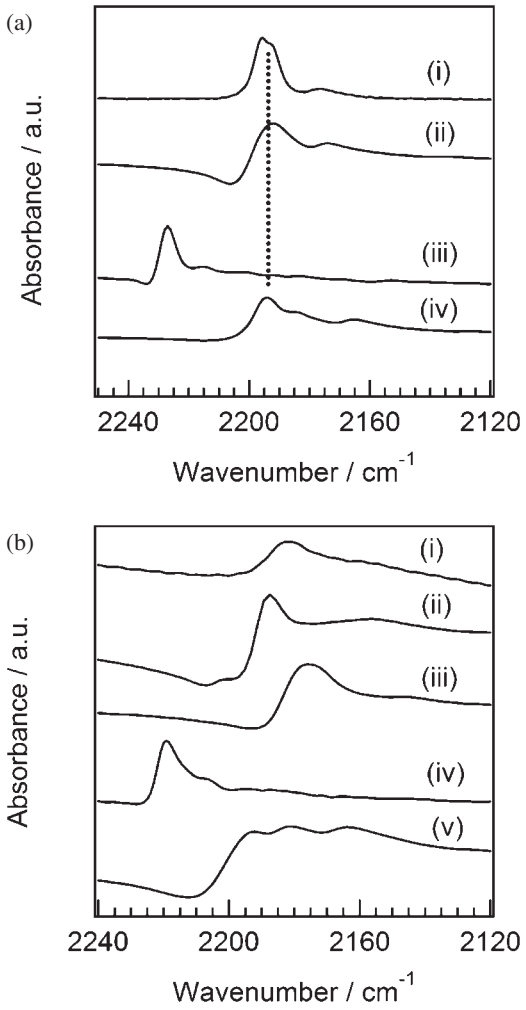

Figure 4. Vibrational spectra at the energy region of ν_{CN}-stretching modes. (a) F_4TCNQ system of (i) LB film of **1a**–F_4TCNQ, (ii) crystalline (**1b**)$(F_4TCNQ)_2$, (iii) neutral F_4TCNQ, and (iv) fully ionic $Na^+(F_4TCNQ^{-})$ as KBr pellets. (b) Br_2TCNQ system of (i) LB film of **1a**–Br_2TCNQ, (ii) crystalline (TTF bisannulated [24]crown-8^{2+}) $(Br_2TCNQ^{-2/3})_3$, (iii) crystalline (**1b**)$(Br_2TCNQ)_2$, (iv) neutral Br_2TCNQ, and (v) fully ionic $K^+(Br_2TCNQ^{-})$ as KBr pellets.

ν_{CN}-band (2180 cm^{-1}) of $K^+(Br_2TCNQ^{-})$, the ν_{CN}-bands near 2176 cm^{-1} was assigned to the fully ionic Br_2TCNQ^{-} anion. The similarity between the ν_{CN}-band of **1a**–Br_2TCNQ in the LB film (2182 cm^{-1}) and that of (TTF bisannulated [24]crown-8^{2+}) $(Br_2TCNQ^{-2/3})_3$ (2186 cm^{-1}), which is a partial CT complex of the segregated type,[28] suggests the presence of such partial CT complexes in the **1a**–Br_2TCNQ LB film. Because the energy corresponding to the CN-stretching band was lower than that of **1a**–Br_2TCNQ, the charge on Br_2TCNQ in the LB film should be greater than $-2/3$.

Electrical Conductivity of the LB Films. Whereas the activation energy (E_a) of the LB film of **1a**–Br_2TCNQ (E_a = 0.15 eV, $T > 100$ K) was comparable to that of **1a**–F_4TCNQ (E_a = 0.21 eV, $T > 100$ K), the electrical conductivity (σ_{RT}) of the LB film of **1a**–Br_2TCNQ at rt ($\sigma_{RT} = 1.2 \times 10^{-2}\,S\,cm^{-1}$) was two orders of magnitude higher than that of **1a**–F_4TCNQ

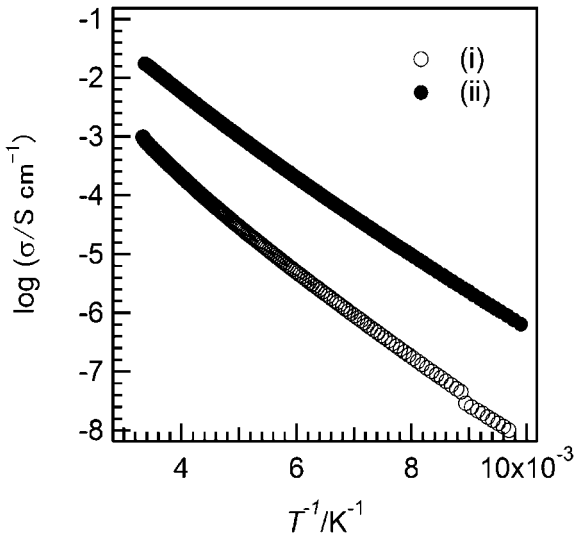

Figure 5. The conductivity behavior of **1a**–F_4TCNQ (i) and **1a**–Br_2TCNQ (ii) in LB films.

($\sigma_{RT} = 3.9 \times 10^{-4}$ S cm^{-1}) (Figure 5). Both LB films showed a semiconducting temperature dependency over a temperature range of rt to 77 K. Whereas the low σ_{RT} value and the semiconducting behavior were consistent with the fully ionic ground state of $(\mathbf{1a}^{2+})(F_4TCNQ^{-1})_2$, intrinsically high conductivity can be expected for the microscopic domains of the partial CT complex in the LB film of **1a**–Br_2TCNQ due to the appearance of the **A**-band. However, neutral **1a** in LB film may strongly prevent the microscopic carrier transport in it, resulting in moderate magnitude of room-temperature conductivity of the **1a**–Br_2TCNQ LB film. The intrinsic conductivity of **1a**–Br_2TCNQ should be one or two order of magnitude higher than the observed value.

Conclusion

CT complexes between ethylenedithio-substituted amphiphilic bis-TTF macrocycle **1a** as the electron donor and TCNQ derivatives as electron acceptors were employed in the construction of electrically-active LB films. The F_4TCNQ and Br_2TCNQ electron acceptors was able to form stable CT complexes with donor **1a**. Based on the AFM images, the corresponding LB films of both complexes afforded relatively uniform surfaces, which can be attributed to the ethylenedithio substituent, and may increase the dimensionality of intermolecular interactions. The electronic spectra of **1a**–F_4TCNQ and **1a**–Br_2TCNQ in the LB films were consistent with those of fully ionic and partial CT electronic ground states, respectively. The difference between the electron affinities of F_4TCNQ and Br_2TCNQ played an important role in the modification of the electronic state of the LB films. XPS, AFM, and optical measurements indicated that the LB film of **1a**–Br_2TCNQ was composed of neutral **1a** and the CT complex between **1a** and Br_2TCNQ. Although the partial CT state of **1a**–Br_2TCNQ was confirmed, temperature-dependent semiconducting properties were observed for **1a**–F_4TCNQ and **1a**–Br_2TCNQ LB films, with σ_{RT} of 3.9×10^{-4} and 1.2×10^{-2} S cm^{-1}, respectively, at rt. Our results show that ethylenedithio-substituted amphiphilic bis-TTF macrocycles can effectively enhance the dimensionality of intermolecular interactions, and allow electrical conducting behavior in the CT complex in nanoscale molecular assemblies. The next step of constructing LB films of pure partial CT complexes by adjusting the strength of acceptor and the substituent of TTF units are currently underway in our laboratories.

This work was partly supported by a Grant-in-Aid for Science Research from the Ministry of Education, Culture, Sports, Science and Technology of Japan.

Supporting Information

Detailed results are available in Supporting Information. This material is available free of charge on the web at http://www.csj.jp/journals/bcsj/.

References

1 K. J. Klabunde, *Nanoscale Materials in Chemistry*, Wiley-Interscience New York, **2001**.
2 Y. Peidong, *The Chemistry of Nanostructured Materials*, World Scientific New Jersey, **2003**.
3 K. Sugiura, M. Matsumoto, H. Tada, T. Nakamura, *Chemistry of Nanomolecular Systems: Towards the Realization of Molecular Devices*, Springer-Verlag Berlin, **2002**.
4 Y. Wu, J. Xiang, C. Yang, W. Li, C. M. Lieber, *Nature* **2004**, *430*, 61.
5 M. C. Petty, *Langmuir–Blodgett Films: An Introduction*, Cambridge University Press Cambridge, **1996**.
6 T. Nakamura, M. Tanaka, T. Sekiguchi, Y. Kawabata, *J. Am. Chem. Soc.* **1986**, *108*, 1302.
7 T. Iyoda, M. Ando, T. Kaneko, A. Ohtani, T. Shimidzu, K. Honda, *Tetrahedron Lett.* **1986**, *27*, 5633.
8 R. M. Metzger, R. R. Schumaker, M. P. Cava, R. K. Laidlaw, C. A. Panetta, E. Torres, *Langmuir* **1988**, *4*, 298.
9 T. Nakamura, *Handbook of Organic Conductive Molecules and Polymers Vol. 1 Charge-Transfer Salts, Fullerenes and Photoconductors*, Wiley Stuttgart, **1997**, p. 728.
10 M. R. Bryce, M. C. Petty, *Nature* **1995**, *374*, 771.
11 R. M. Metzger, *Acc. Chem. Res.* **1999**, *32*, 950.
12 H. Tachibana, T. Nakamura, M. Matsumoto, H. Komizu, E. Manda, H. Niino, A. Yabe, Y. Kawabata, *J. Am. Chem. Soc.* **1989**, *111*, 3080.
13 D. O. Cowan, *New Aspects of Organic Chemistry*, Kodansha Tokyo, **1989**.
14 T. Akutagawa, T. Ohta, T. Hasegawa, T. Nakamura, C. A. Christensen, J. Becher, *Proc. Natl. Acad. Sci. U.S.A.* **2002**, *99*, 5028.
15 T. Akutagawa, K. Kakiuchi, T. Hasegawa, T. Nakamura, C. A. Christensen, J. Becher, *Langmuir* **2004**, *20*, 4187.
16 T. Nakamura, Y. Tatewaki, T. Ohta, K. Wakahara, T. Akutagawa, T. Hasegawa, H. Tachibana, R. Azumi, M. Matsumoto, C. A. Christensen, J. Becher, *Bull. Chem. Soc. Jpn.* **2005**, *78*, 247.
17 T. Nakamura, H. Miyata, K. Wakahara, T. Akutagawa, T. Hasegawa, H. Hasegawa, S. Mashiko, C. A. Christensen, J. Becher, *J. Nanosci. Nanotechnol.* **2006**, *6*, 1833.
18 T. Akutagawa, K. Kakiuchi, T. Hasegawa, S. Noro, T. Nakamura, H. Hasegawa, S. Mashiko, J. Becher, *Angew. Chem., Int. Ed.* **2005**, *44*, 7283.
19 T. Akutagawa, G. Saito, M. Kusunoki, K. Sakaguchi, *Bull. Chem. Soc. Jpn.* **1996**, *69*, 2487.

20 T. Akutagawa, Y. Abe, Y. Nezu, T. Nakamura, M. Kataoka, A. Yamanaka, K. Inoue, T. Inabe, C. A. Christensen, J. Becher, *Inorg. Chem.* **1998**, *37*, 2330.

21 T. Akutagawa, Y. Abe, T. Hasegawa, T. Nakamura, T. Inabe, C. A. Christensen, J. Becher, *Chem. Lett.* **2000**, 132.

22 J. B. Torrance, J. J. Mayerle, K. Bechgaard, B. D. Silverman, Y. Tomkiewicz, *Phys. Rev. B* **1980**, *22*, 4960.

23 T. Akutagawa, G. Saito, *Bull. Chem. Soc. Jpn.* **1995**, *68*, 1753.

24 G. Saito, J. P. Ferraris, *Bull. Chem. Soc. Jpn.* **1980**, *53*, 2141.

25 J. B. Torrance, J. E. Vazquez, J. J. Mayerle, V. Y. Lee, *Phys. Rev. Lett.* **1981**, *46*, 253.

26 M. Meneghetti, A. Girlando, C. Pecile, *J. Chem. Phys.* **1985**, *83*, 3134.

27 M. Meneghetti, C. Pecile, *J. Chem. Phys.* **1986**, *84*, 4149.

28 Y. Abe, T. Akutagawa, T. Hasegawa, T. Nakamura, K. Sugiura, Y. Sakata, T. Inabe, C. A. Christensen, J. Becher, *Synth. Met.* **1999**, *102*, 1599.